European Journal of Medicinal Chemistry 57 (2012) 362–372

Contents lists available at SciVerse ScienceDirect

European Journal of Medicinal Chemistry

journal homepage: http://www.elsevier.com/locate/ejmech

Original article

Design of new arylamino-2-ethane-1,1-diyl- and benzoxazole-2-methylene-bisphosphonates *vs* cytotoxicity and chronic inflammation diseases. From hydrophobicity prediction to synthesis and biological evaluation

Wafaa M. Abdou [a,*], Reham F. Barghash [a], Ashraf A. Sediek [b]

[a] Chemical Industries Division, National Research Centre, Elbohouth St., D-12311 Dokki, Cairo, Egypt
[b] Chemistry Department, Faculty of Sciences and Arts, Al-Kamil Branch, King Abdulaziz University, Jeddah, Saudi Arabia

ARTICLE INFO

Article history:
Received 26 June 2012
Received in revised form
19 September 2012
Accepted 24 September 2012
Available online 2 October 2012

Keywords:
Bisphosphonates
Bisphosphonic acids
Benzoxazoles
Antitumor activity
Antichronic inflammation
Lipophilicity measurement

ABSTRACT

A general synthetic approach to two new series of methylenebisphosphonates: arylamino-2-ethane-1,1-diyl- and benzoxazole-2-methylenebisphosphonates is presented. Acid hydrolysis of selected BPs was undertaken to give the corresponding bisphosphonic acid (BP-acid). Next, the prediction of the permeability (hydrophobicity) of the target compounds was measured, by a combination of RP-HPLC and computational techniques, to study the capacity of transporting the molecule through cellular membranes. Cytotoxicity/growth inhibition of 50% (GI_{50}, mg/L) and antichronic inflammation properties of the products were evaluated. Later on, a comparison of the pharmacological results with water −octanol partition coefficients (log K_{OW}) of the compounds was also reported.

1. Introduction

Bisphosphonates (BPs) are very powerful inhibitors of bone resorption and their main therapeutic use being in diseases with high bone turnover such as Paget's disease and osteoporosis [1–5]. This strong affinity of BPs for bone minerals allows the rapid and selective targeting of bone in vivo [5–8]. In addition to inhibiting bone resorption, BPs have also been shown to exhibit antiinflammatory and antitumor effects. In vivo, BPs inhibit proliferation and induce apoptosis in cultured human breast cancer cells, and in turn the chance of development of metastases is much less [9–13].

Bone is a common site of breast and prostate cancer metastasis. Metastatic bone disease is, however, often associated with bone pain, pathologic fractures, and nerve compression syndromes. Such complications result in decreasing the quality of life [9]. Unfortunately, until now there is no cure for patients with bone metastasis. Therefore, effective therapies to inhibit the progression of bone metastasis would have important clinical benefits. The ideal drug delivery system is thought to be one that restricts its pharmacological activity solely to target sites. Thus, if the drug or delivery vehicle has a high affinity for only bone tissue, its therapeutic effect on bone related disease is maximized and its distribution to other sites is minimized. Hydroxyapatite [HA, $Ca_{10}(PO_4)_6(OH)_2$] is the major inorganic mineral phase found in bone and teeth, and it is not present in other tissue under normal circumstances, therefore, targeting drug delivery to HA is expected to result in a sole delivery to bone tissue. In sequel, BPs, which are considered to be analogs of endogenous pyrophosphate, have a significant affinity for HA could be excellent effective therapies for inhibiting the progression of bone metastasis. Notwithstanding, the cellular and biochemical mechanisms of action of BPs are yet to be completely unraveled, nevertheless, over the last two decades, there was a significant progress in elucidating the mechanism of action of BPs, which in general can shorten the life span of osteoclasts by inducing programmed cell death (apoptosis). Moreover, some important structure activity relationship (SAR) trends of this class of agents have emerged [14,15], e.g., by incorporating a hydroxyl group and/or amino group close from $-CP_2$, increases the affinity to hydroxyapatite, by at least 10 fold [1,3].

In a previous work, we reported the synthesis of a series of tetrazoloquinoline-based ethylene bisphosphonic acids of remarkable antitumor activity against breast (especially MDA-MB-23/ATCC), and prostate cancer (PC-3 and DU-145) [16]. Later on, we extended this work and a series of substituted isoquinoline-bisphosphonates

* Corresponding author. Tel.: +20 233371615; fax: +20 233370931.
E-mail addresses: wabdou@link.net, wabdou@intouch.com (W.M. Abdou).

0223-5234/$ – see front matter © 2012 Elsevier Masson SAS. All rights reserved.
http://dx.doi.org/10.1016/j.ejmech.2012.09.032

of potent and promising antineoplastic activity was prepared. Four BPs cause a dose dependent increase in sister chromatid exchange (SCE) frequency followed by a decrease of proliferation rate [17]. A group of heterocyclic-*N*, *S*-BPs of more proliferation rate index (PRI) compared to the control drug were recently reported to compare their chemistry and their activity with that of their oxygen counterparts as antitumor agents [18]. In view of the above mentioned facts and in continuation of our interest in both chemistry and biological activities of BPs, it was of interest to prepare two series of methylenebisphosphonates: arylamino-2-ethane-1,1-diyl- and benzoxazole-2-methylene-bisphosphonates and their relevant BP-acids to evaluate their antitumor- and chronic inflammation properties. The approach is based on the application of methylenebisphosphonate reagent, **5** to a group of Schiff-bases, **4a**–**i**. Lipophilicity (permeability) of the studied compounds was measured before the pharmacological evaluation. Drugs cross biological barriers most frequently through passive transfer, which strongly depends on their lipophilicity. The prediction of the permeability, which expresses the transport of the molecule through cellular membranes is therefore, considered one of the most important physical properties of biologically active compounds [19,20].

2. Chemistry

The required Schiff bases, **4a**–**i** were generated in high yields from the condensation of 2-aminophenol **2** with the appropriate aromatic aldehydes **3a**–**i**. However, 2-amino-4,6-di-tert-butylphenol, **2** is not commercially available, and was therefore synthesized by aminolysis of the parent 3,5-di-tert-butyl-1,2-benzoquinone (**1**, Scheme 1) [21,22]. The reaction procedures for preparing the target diphosphonate derivatives as well as the course of the reactions were depicted in Schemes 2–4.

The substrates **4a**–**d** was treated with phosphorus reagent, **5** in ethanol solution containing EtONa. The reaction mixture was stirred at r.t. for the proper time (TLC) to give, after the usual workup, tetraethyl 2-(3,5-di-tert-butyl-2-hydroxyphenylamino)-2-(aryl)ethane-1,1-diyl-diphosphonates, **6a**–**d** as major products (~71%) together with tetraethyl (5,7-di-tert-butyl-2-(aryl)-2,3-dihydrobenzo[doxazol-2-yl) methylenediphosphonates, **7a**–**d** (≤7%). Obviously, nucleophilic addition of the methylene-C in **5** to the imino-C of **4** gave rise to the products **6a**–**d**. Nevertheless, slight homo-oxidation of **6** resulted in the formation of oxazoles **7** via an intramolecular cyclization in tandem of extrusion of a hydrogen molecule. The latter process was previously discussed for the transformation of 3,5-di-tert-butyl-2-hydroxyphenylamino derivatives to the corresponding benzoxazoles [21]. Furthermore, when the above reaction [**4** + **5**] was allowed to proceed in methanol solution containing MeONa and catalytic amount of 2,3-dichloro-5,6-dicyano-benzoquinone (DDQ) [23] oxazoles **7a**–**d** were obtained as enantiomer products in ≈75% yields.

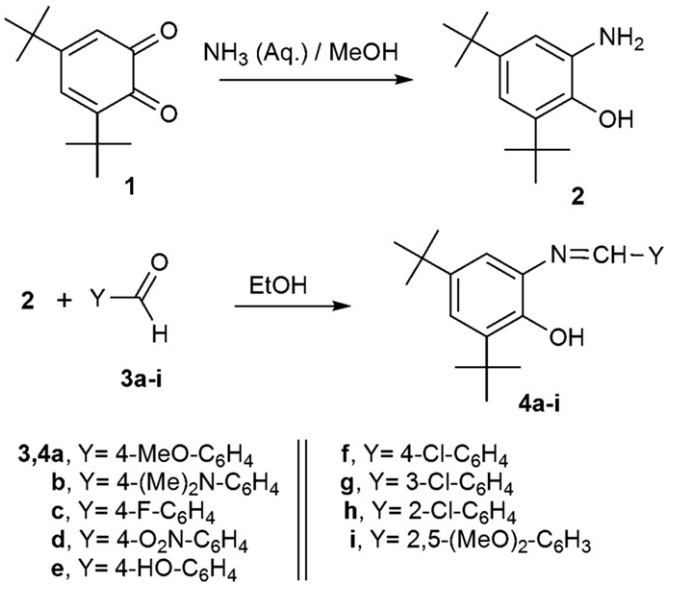

Scheme 1. Synthesis of Schiff-bases **4a**–**i**.

Identification of structures **6** and **7** was confirmed by combustion analysis, MS, IR, and NMR-spectroscopy. Compounds **6a**–**d** [$\delta_P \approx 30$, 25 (2d, $J_{P-P} = 26.4$ Hz)] have sharp melting points and did not show any isomerism in the spectroscopic data. The ^{1}H NMR (500.6 MHz) of **6a** revealed two types of methine protons with two different chemical shifts at 3.73 (dt, $J_{H-H} = 9.3$, $^2J_{P-H} = 14.4$ Hz, H^aC–P_2) and 4.88 (dt, $^3J_{H-H} = 9.3$, $^3J_{P-H} = 6.2$ Hz, H^b–C*–Y). This large coupling constant (J_{H-H}) of H^b with H^a indicates that H^a is in anti-configuration to H^b-C*. The enantiospecific isomer **6** was also verified by careful inspection of a model in terms of the Newman projection, which confirmed the staggered *anti*-conformation of H^b and H^a.

On the other hand, oxazole-2-methylenediphosphonate **7a** was analyzed correctly for $C_{31}H_{49}NO_8P_2$: *m*/*z* (%): 624 (17) [$M^+ - 1$]. In the NMR spectra of **7a**, the presence of the exocyclic methine moiety (CH–P_2) was found at δ_H 3.06 (t, $^2J_{P-H} = 16.8$ Hz) and at δ_C 38.7 (t, $^1J_{P-C} = 168.3$ Hz). These data excluded any possible cyclization reaction involving the methylenediphosphonate moiety (structure **8**), and confirmed that the intramolecular cyclization proceeded via the other HC-Y-moiety.

In contrast to the above result, applying the reagent **5** to the Schiff bases **4e**–**i** in MeONa solution at r.t., using the same amounts did not show any appreciated reaction, and the starting material **4e**–**i** was recovered practically unchanged. However, the reactions between **4e**–**i** and **5** were completed smoothly, only on heating the reaction mixture under reflux temperature and in the presence of DDQ in the medium, to yield the respective oxazole-2-methylenediphosphonates **7e**–**i** (≈76%) (Scheme 3).

Recent advances in pharma laboratories have impressively identified remarkable therapeutics from 1,1-bisphosphonic acid to 1,1-bisphosphonate ester counterparts [1]. Consequently, based on evaluation results of the permeability of the synthesized BPs, hydrolysis of representative BPs **6b**,**c**, **7b**,**c**, and **7f**–**h** was undertaken to give the corresponding BP-acids **9a**,**b** and **10a**–**e** (Scheme 4).

The structures suggested for all new compounds are in good agreement with their analytical and spectral data (see Experimental section).

3. Pharmacological evaluation

3.1. Prediction and lipophilicity

Hydrophobicity is one of the most important physical properties of biologically active compounds. This thermodynamic parameter describes the partitioning of a compound between an aqueous and an organic phase and is characterized by the partition coefficient (log *P*). Reversed phase high performance liquid chromatography (RP-HPLC) methods have become popular and are widely used for lipophilicity measurement [19,20]. The general procedure consists of the measurement of the directly accessible retention time under isocratic conditions with varying amounts of an organic modifier in the mobile phase using end-capped non-polar C18 stationary RP columns and calculating the capacity factor *K*. Log *K*, calculated from the capacity factor *K*, is used as the lipophilicity index and then converted to log *P* scale [24].

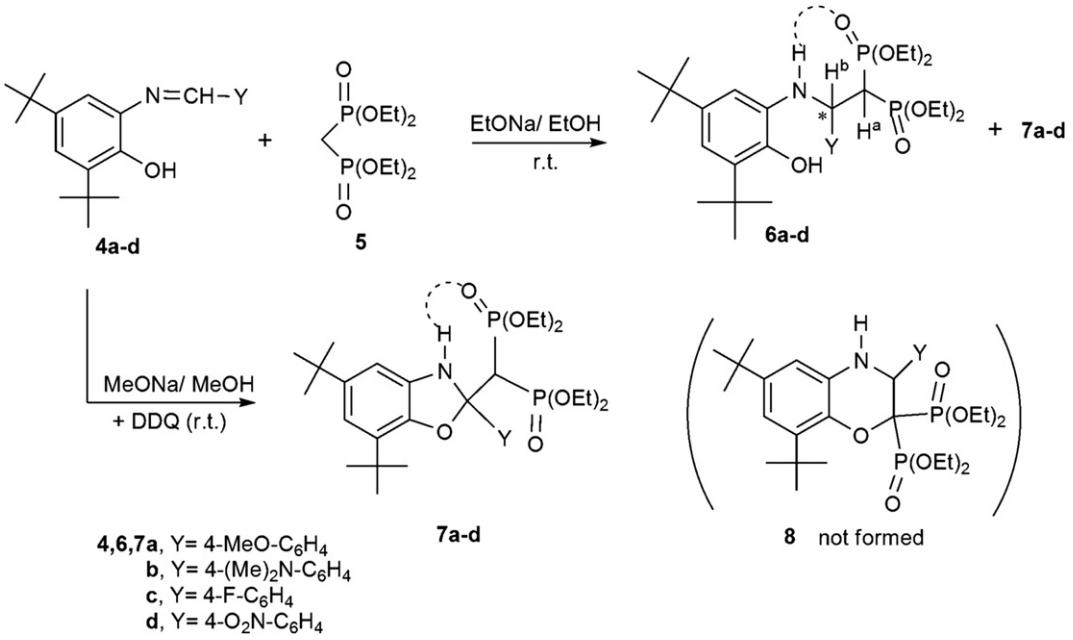

Scheme 2. Synthesis of BPs **6a**–**d** and **7a**–**d**.

Hydrophobicities of the new compounds **6a**–**d**, **7a**–**i**, **9a**,**b**, and **10a**–**e**, Log *P*, *i.e.* the logarithm of the partition coefficient for *n*-octanol/water, was calculated using the programs CS ChemOffice Ultra ver. 9.0 (CambridgeSoft, Cambridge, MA, U.S.A., Clog *P*) and ACD/LogP ver. 1.0 (Advanced Chemistry Development Inc. Toronto, Canada), softwares. The results are shown in Table 1. The displayed data showed that the experimentally determined log *K* values correlate relatively poorly with all computed lipophilicity data using ACD/Log *P* program. Nevertheless, log *P* values calculated by the ChemOffice software (Clog *P*) agree better with both targets BPs and BP-acids. On the other hand, obviously, the dimethoxy substituent **7i** possessed, as expected, the lowest lipophilicity (log *K*) while the phenolic *N*-BP-acid, **9a** showed the highest lipophilicity. Generally, BP-acid series has higher measured permeability than their BP-counterparts. Also, amino-substituted BPs **6a**–**d** display, in contrast with our expectations, better hydrophobicities (log *P*/Clog *P* values) than the corresponding oxazole analogs. Nevertheless, looking insight one series, e.g., oxazole-BPs **7a**–**i**, the substituent effect on the activity is in the order of: dimethylamine **7b** > flouro **7c** > hydroxyl **7e** > chloro **7f**–**h** > methoxy **7a** > nitro **7d** > dimethoxy **7i**. Finally, only slight differences were observed in the permeability's (log *K*) between the isomers **7f**, **7g** or **7h** of the same substituent (Cl) in one molecule.

3.2. Biological assessment

3.2.1. Antitumor activity screening

Antitumor activity of selected BPs **6b**,**c**, **7b**,**c** and BP-acids **9a**,**b** and **10a**–**c** was carried out at a dose of 10 μM utilizing 16 different human tumor cell lines; representing breast, ovarian, prostate, as well as liver, according to the previously reported standard method [24,25]. Substrates **4a** and **4g** were also biologically tested in a trial to reflect the effect of introducing BP-moiety.

The results were displayed in Table 2 and showed an interesting activity for several compounds. For the purpose of the study, cell line growth inhibition with >50% at a concentration of 10 μM was considered to be a noticeable activity. Other than the substrates **4a** and **4g**, all synthesized compounds reflect remarkable antitumor activity against breast (especially MDA-MB-231/ATCC and BT-549), and prostate carcinoma cell lines (PC-3 and DU-145), whereas a moderate to good effect was observed on ovarian and liver cancer cells. The four most active compounds are **9a** > **9b** > **10a** > **6b**. SARs correlation for these reported observations revealed that the presence of dialkylamino group as a substituent to the aryl-moiety is usually associated with the enhancement in antitumor properties as indicated in compounds **6b**, **7b**, **9a**, and **10a**. Furthermore, the data showed that the BP-acid series has higher activity than their

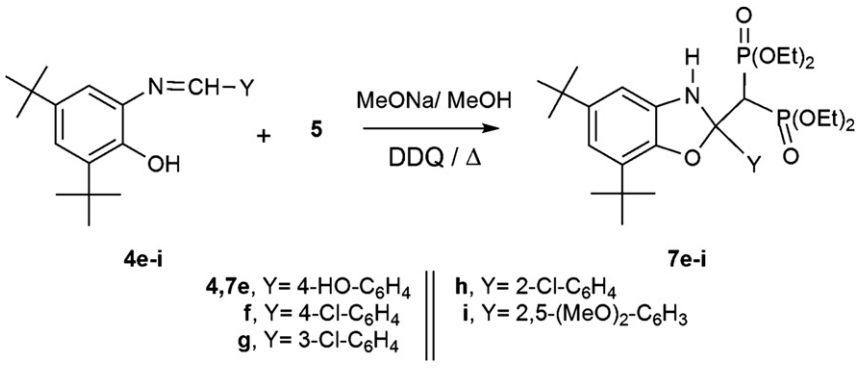

Scheme 3. Synthesis of BPs **7e**–**i**.

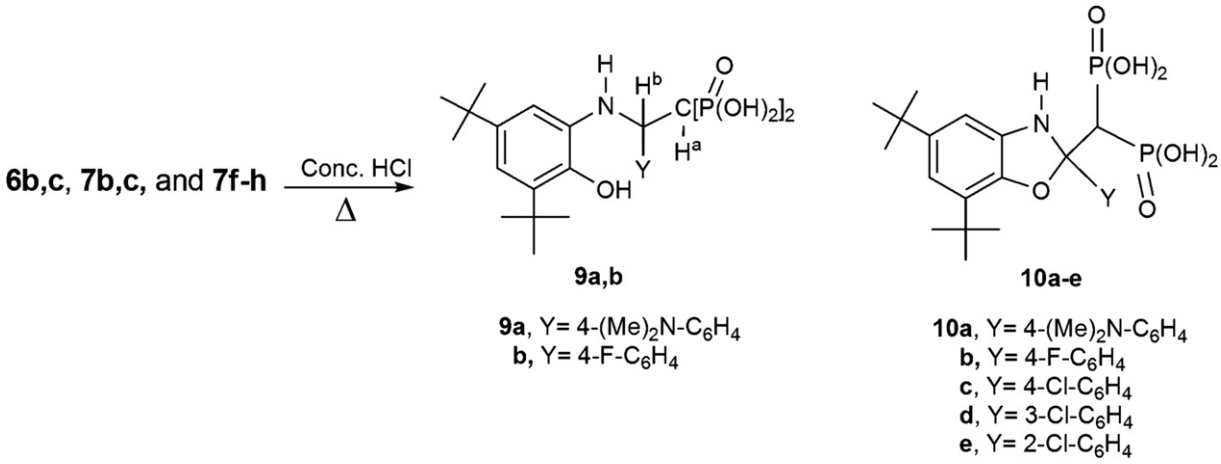

Scheme 4. Synthesis of BP-acids **9a**,**b** and **10a**–**e**.

BP-counterparts. Finally, it could be assumed, in general, that the four compounds of the most antitumor activity are the same of the highest lipophilicity. However, a straight correlation between the activity and lipophilicity of BPs or BP-acids was not found, and the antitumor activity seems to be independent of lipophilicity and dependent on chemical structure. Further studies on experimental tumors in vivo for evaluating the possible antineoplastic potential of the most promising compounds are in progress.

3.2.2. Antiinflammatory screening

The in vivo antiinflammatory activity of all BP-products, **6a**–**d** and **7a**–**i**, as well as BP-acids **9a**,**b** and **10a**–**e** was determined by using a delayed-type hypersensitivity granuloma model [26], and were compared with that of the BP-drug, risedronate, **11** at the same dose. The substrates **4a** and **4g** were also tested to reflect the effect of introducing the phosphorus moiety. BP-**11** was selected for its optimal potency and safety in early screening of similar assays [1]. Furthermore, this model is unaffected by traditional nonsteroidal antiinflammatory drugs, such as indomethacin, aspirin or ibuprofen [27].

A delayed-type hypersensitivity granuloma assay is a model of chronic inflammation, in which mice were previously sensitized to methylated bovine serum albumin (mBSA) and subjected to surgical implantation of sc in the dorsum of the mice in order to generate granuloma. All compounds were prepared as solutions or emulsions and the pH was adjusted to 7.4. Each mouse received the tested compound in a volume of 0.l/10 g of body weight sc in the scruff of the neck. Dosing (25–100 mg/kg) commenced on the day of implantation of the soaked discs and was continued thereafter on a daily basis until day nine, when the mice were euthanized. The granulomatous lesions were then excised and measurements were taken for both wet and dry tissue weights. The data is displayed in Table 3 and Fig. 1. The results were analyzed by Student's paired *t* test. Structure 11

Table 1
Comparison of the determined log *K* values with the calculated lipophilicity (log *P*/Clog *P*) and ACD/LogP ver. 1.0, of **6a**–**d**, **7a**–**i**, **9a**,**b**, and **10a**–**e**.

Cpd	Y	Log *P* (Clog *P*/ ChemOffice)	Log *P* ACD/LogP ver. 1.0
6a	4-MeO–C_6H_4	7.49/3.06544	7.05 ± 0.51
6b	4-$(Me)_2$N–C_6H_4	8.01/3.31144	7.24 ± 0.52
6c	4-F–C_6H_4	7.88/3.28944	7.18 ± 0.57
6d	4- O_2N–C_6H_4	NT/2.88944	6.86 ± 0.51
7a	4-MeO–C_6H_4	8.19/4.92904	6.70 ± 0.73
7b	4-$(Me)_2$N–C_6H_4	8.71/5.17504	6.90 ± 0.73
7c	4-F–C_6H_4	8.58/5.15304	6.84 ± 0.77
7d	4-O_2N–C_6H_4	NT/4.75304	6.52 ± 0.73
7e	4-HO–C_6H_4	8.16/3.43404	6.05 ± 0.73
7f	4-Cl–C_6H_4	8.96/5.72304	7.38 ± 0.73
7g	3-Cl–C_6H_4	8.96/5.72304	7.38 ± 0.73
7h	2-Cl–C_6H_4	8.96/5.72304	7.38 ± 0.73
7i	2,5-MeO–C_6H_4	7.94/5.01804	6.67 ± 0.75
9a	4-$(Me)_2$N–C_6H_4	6.51/0.7106	2.63 ± 0.72
9b	4-F–C_6H_4	6.38/0.68864	2.57 ± 0.76
10a	4-$(Me)_2$N–C_6H_4	7.21/2.57424	2.29 ± 0.89
10b	4-F–C_6H_4	7.08/2.55224	2.23 ± 0.92
10c	4-Cl–C_6H_4	7.46/3.12224	2.78 ± 0.88
10d	3-Cl–C_6H_4	7.46/3.12224	2.78 ± 0.88
10e	2-Cl–C_6H_4	7.46/3.12224	2.78 ± 0.88

The data in Table 3 shows that **11** reproducibly inhibited granuloma wet- and dry weights and served as a positive control in other experiments. Other than the substrates **4a** and **4g**, ten of twenty tested new compounds have moderate to good antiinflammatory properties when compared with the standard drug **11**, without toxic side-effects toxicity (evaluation result is provided as Supplementary document). Compounds **6b**,**c**, **7b**,**c**, and **7f**–**h** significantly inhibited the granuloma in a dose-dependent manner, while **6d**, **9a**, and **9b** displayed an inhibitory effect, which is almost equivalent to that of risedronate at 100 mg/kg. BPs **6**a, **7i**, and BP-acids **10a**–**c** showed marginal activity against the dry weight granuloma. In contrast, the substrates **4a** and **4g** were inactive at all doses.

Structure-activity correlation based on the obtained results indicates that the presence of the bisphosphonate moiety is an essential factor in developing the total pharmacological properties for these compounds. Compounds **6b**,**c** **7b**,**c**, and **7f**–**h** are the most active structures among all products, and the presence of the free or alkylatedamino group highly enhanced the efficacy of the compounds, **6b**, **7b**, **9b**, and **10b**. In contrast, introducing the two methoxy groups at the phenyl moiety (e.g., see compound **7i**) results incomplete loss of the activity. Conversion of **6b** and **6c** to the corresponding bisphosphonic acids **9a** and **9b** results in decreasing the activity. This observation is not surprising as it is previously reported in similar occasions [26]. The results of the bioassay also indicate that the activity of the tested BPs on chronic inflammation is dose dependent. Finally, the results also show that the experimentally determined log *K* values (Table 1) are in moderate agreement with the antiinflammatory properties for the same compounds.

4. Conclusion

In summary, the present investigation offered two new series of BPs: 2-hydroxyphenylamino-2-ethane-gem-diphosphonates and

Table 2
Concentrations resulting in growth inhibition of 50% (GI_{50}, mg/L) of *in vitro* human tumor cell lines of **6b**,**c**, **7b**,**c**, **9a**,**b**, and **10a**–**c**.

Panel/cell line	Compounds									
	4a/**4g**	**6b**	**6c**	**7b**	**7c**	**9a**	**9b**	**10a**	**10b**	**10c**
Breast cancer										
McF7	> 46	17.3	26.80	14.88	25.21	8.40	15.7	9.80	14.58	10.64
NCl/ADRRES	> 46	18.32	9.37	17.8	20.1	6.20	6.45	6.80	12.41	18.05
MDA-MB-231/ATCC	> 46	10.6	11.93	12.74	14.72	4.83	5.68	8.9	10.12	11.5
HS578T	> 46	14.80	26.92	26.10	24.2	8.92	10.6	20.2	8.36	24.12
MDA-MB-435	> 46	14.60	18.08	16.02	16.4	5.32	9.85	8.84	13.4	14.5
BT-549	> 46	13.3	18.13	5.05	11.97	5,05	14.6	NT	32.1	NT
T-47D	> 46	14.06	14.12	17.05	22.18	11.08	11.65	13.57	13.42	13.55
Ovarian cancer										
IGROVI	> 46	15.3	14.8	20.2	26.1	7.9	11.6	16.8	20.6	24.8
OVCAR-3	> 46	7.41	11.4	16.55	18.9	4.4	7.4	14.5	10.7	NT
OVCAR-4	> 46	9.8	10.6	10.18	10.52	3.6	4.32	4.83	8.65	10.18
OVCAR-5	> 46	16.5	25.6	17.8	NT	30.6	16.3	10.3	40.04	36.6
OVCAR-8	> 46	14.06	28.4	21.41	NT	11.4	13.5	12.66	13.7	28.6
SK-OV-3	> 46	16.5	16.76	14.46	17.13	11.53	13.6	12.6	13.68	16.5
Prostate cancer										
PC-3	> 46	6.98	8.6	14.2	14.2	3.82	5.6	10.82	19.6	>52
DU-145	> 46	6.54	9.42	11.23	11.6	2.38	4.52	8.75	15.3	10.5
Liver cancer										
HEPG2	> 50	7.96	7.97	15.5	16.7	3.16	3.42	8.52	24.23	32.42

NT: not tested.

benzoxazole-2-methaylenediphosphonates as antitumor and anti-inflammatory drugs. We have also attempted in this research work to utilize the high bone specificity of BP-acids with other chemical moieties of potential anticatabolic pharmacology to test the new compounds for treating tumor proliferation diseases. The obtained results indicated percentage growth inhibition of 50% (GI_{50}, mg/L) for several new BP-acids.

Biological evaluation versus chronic inflammation was also tested whereby the screening result indicated the presence of free phenolic (OH), amine and/or alkylatedamino group in the BPs would enhance their potency. These groups may facilitate the binding to the metal atom in the active site of the matrix metalloproteinases (MMPs) [19,20]. In parallel, the hydrophobicity evaluation of the target compounds was tested as a prediction and prerequisite for pharmacological screening and drug development. The prediction of the measured permeability (lipophilicity) was measured by means of RP-HPLC and a computational technique was also reported in this communication. Unfortunately, the results showed that the experimentally determined log *K* values (Table 1) correlate relatively poorly with the evaluated pharmacological potency.

5. Experimental section

Melting points (uncorrected) were determined with open capillary tube on an Electrothermal (variable heater) melting point apparatus. IR spectra were recorded on a JASCO FT-IR 6100 using KBr disc. NMR spectra were measured with a JEOL E.C.A-500 MHz (^{13}C: 125.8 MHz, ^{1}H: 500.6 MHz, ^{31}P: 200.7 MHz) spectrometer. ^{31}P NMR spectra were recorded with H_3PO_4 (85%) as external reference. ^{1}H and ^{13}C NMR spectra were recorded with trimethylsilane as internal standard in $CDCl_3$ or DMSO-d_6. Chemical shifts (δ) are given in ppm. The mass spectra were performed at 70 eV on an MS-50 Kratos (A.E.I.) spectrometer provided with a data system. The appropriate precautions in handling moisture-sensitive compounds were observed. The purity of all new samples was verified by microchemical analysis (H/C/N/P) and spectroscopy. Solvents were dried by standard techniques. TLC: Merck 0.2 mm silica gel 60 F254 analytic aluminum plates. Column chromatography (CC): silica gel (Kieselgel 60 mesh, particle size 0.2–0.5 mm; E. Merck, Darmstadt). All international principles and local regulations concerning the care and use of laboratory animals were considered during the pharmacological screening. The substrates **4a**–**i** were prepared according to the reported method [21,22].

5.1. General procedure of bisphosphonates (BPs) *6a–d* and *7a–d*

A solution of 4.2 mmol of tetraethyl methylenebiphosphonate, **5** in 10 mL of absolute ethanol containing 9.12 mmol sodium (Na) was stirred at 0 °C for about 0.5 h. A solution of 3.8 mmol of the Schiff-base **4a**–**d** in 10 mL of EtOH was then added in one portion, and the reaction was stirred at r.t., for ≈12 h (TLC). The product mixture was cooled, poured into ice-water, and acidified with conc HCl to pH ≈6, followed by extraction with AcOEt (3 × 50 mL), and the combined organic phase was dried over *anh*. Na_2SO_4. After removal of the volatile materials under vacuum, the resulting residue was chromatographed on silica gel with *n*-hexane/$CHCl_3$ to give the respective BPs **6a**–**d** and **7a**–**d**.

5.2. Reaction of *4a* with *5*

Reagents: (*E*)-2,4-Di-tert-butyl-6-(4-methoxybenzylideneamino) phenol, **4a** (1.3 g, 3.8 mmol), BP-reagent **5** (1.2 mL, 4.2 mmol), EtONa (0.2 g of Na, 9.1 mmol), and EtOH (20 mL). The product residue was chromatographed with *n*-hexane/$CHCl_3$ (6:4 v/v) to give **7a**, followed with (1:1 v/v) to give **6a**.

5.2.1. Tetraethyl (5,7-di-tert-butyl-2-(4-methoxyphenyl)-2,3-dihydrobenzo[d]oxazol-2-yl)methylenediphosphonate, *7a*

Colorless crystals, yield: ≈7%, mp 152–154 °C (from CH_2Cl_2). IR (cm^{-1}, KBr): ν_{max} 3334$_w$ (NH), 1235, 1221 (2P=O, bonded), 1179, 1064 (2P–O–C). ^{1}H NMR [$CDCl_3$] ppm: 1.26, 1.34 (2dt, J_{H-H} = 6.6, $^{4}J_{P-H}$ = 4.6 Hz, 2× 6H, 4H_3CCOP), 1.35, 1.40 (2s, 2× 9H, 2(H_3C)$_3$C), 3.06 (t, $^{2}J_{P-H}$ = 16.8 Hz, 1H, *H*C–P$_2$), 3.46 (s, 3H, H_3CO), 4.14, 4.24 (2dq, J_{H-H} = 6.6, $^{3}J_{P-H}$ = 7.2 Hz, 2× 4H, 4H_2COP), 7.15–7.68, 8.27 (m, 6H, *H*–Ar), 8.88 (s (br), 1H, *H*N). ^{13}C NMR [$CDCl_3$] ppm: 158.4, 146.2, 137.4, 134.8, 133.3, 127.1, 122.3, 118.6, 116.5, 110.5 (*C*–Ar), 61.2 (d, $^{2}J_{P-C}$ = 10.5 Hz, *C*H$_2$OP), 55.2 (*C*H$_3$O), 38.7 (t, $^{1}J_{P-C}$ = 168.3 Hz, *C*–P$_2$), 37, 31.7 (2*C*(CH$_3$)$_3$), 31.2, 30.4 (2(*C*H$_3$)$_3$C), 15.4 (d, $^{3}J_{P-C}$ = 7.5 Hz, *C*H$_3$COP). ^{31}P NMR [$CDCl_3$] ppm: 24.3, 28.6 (2d, $^{2}J_{P-P}$ = 24.4 Hz, P_2–C). EI-MS: in *m*/*z* (%): 624 (17) [M^+ − 1], 593 (36) [M^+ − 32(H + OMe)], 319 (48) [M^+ − 306 (H + OMe + 2

Table 3
Delayed-type hypersensitivity granuloma results of BPs **6a**–**d**, **7a**–**i**, and BP-acids **9a**,**b** and **10a**–**e**.

No	Dose (mg/kg) sc[b]	[% Inhibtn/granuloma		Potency(%) dose (100 mg/kg (dry)	Lipophicity prediction log *K*	Coincidence *P*/*E*[c]
		Dry wt	Wet wt			
11	100	48***[a]	44***	100	–	–
	60	44**	40			
	25	33	30			
6a	100	46***	40***	95.8	0.5726	–/+[d]
	60	42**	34*			
	25	30	22			
6b	100	55***	42*	114.6	0.9981	+/+
	60	53	43			
	25	42	30			
6c	100	50**	41***	104.2	0.9254	+/+
	60	45	33			
	25	38	23			
6d	100	45*	42**	93.8	0.5331	–/+
	60	50	28			
	25	36	25			
7a	100	32***	25**	66.7	0.5044	–/–
	50	16	15			
7b	100	49*	44***	102.1	0.8445	+/+
	60	38	32			
	25	22	13			
7c	100	44**	40**	91.7	0.7515	+/+
	60	37	28			
	25	24	20			
	–	–	–			
7d	100	32**	24*	66.7	0.4065	–/–
	50	22	19*			
7e	100	42***	36*	87.5	0.6972	–/+
	50	30	23			
7f	100	41**	36*	85.4	0.6723	–/+
	50	32	21			
7g	100	40**	24*	83.3	0.8507	+/+
	50	30	20			
7h	100	40*	34*	83.3	0.8445	+/+
	50	28	21			
7i	100	18*	16*	37.5	0.3281	–/–
	50	14	10			
9a	100	42***	33**	87.5	1.0021	+/+
	50	29	< 10			
9b	100	44***	34***	91.7	1.0005	+/+
	60	40	31			
	25	32	22			
10a	100	38**	33**	79.2	0.9245	+/+
	50	26	18			
10b	100	44***	39**	91.7	0.9118	+/+
	50	33	24			
10c	100	30*	28**	62.5	0.8543	+/–
	50	24	18			
10d	100	31*	30**	64.6	0.8555	+/–
	50	26	20			
10e	100	30*	30**	62.5	0.8478	+/–
	50	27	21			
4a	100	15**	30**	31.3	–	–
	50	12	16			
4g	100	<10**	<10**	–	–	–
	50	<10	<10			

[a] (***) $p < 0.001$, (**) $p < 0.01$, (*) $p < 0.05$; p is the percentage of inhibition.
[b] sc: subcutaneously.
[c] (*P*/*E*): *P* – prediction (lipophilicity); *E* – experiment (antiinflammatory); *P*/*E* – accuracy of prediction.
[d] +/+ means that both lipophilicity prediction and antiinflammatory give positive results; –/– means that both lipophilicity prediction and antiinflammatory give negative results; +/– means that the lipophilicity prediction gives positive result but antiinflammatory gives negative results; –/+ means that the lipophilicity prediction gives negative results but antiinflammatory gives positive results.

[P(O)(OEt$_2$)]), 306 (100) [M$^+$ – 319 (H + OMe + CH [P(O)(OEt$_2$)$_2$]$_2$)], 287 (58) (CH[P(O)(OEt$_2$)$_2$]$_2$), 137 (46) (P(O)(OEt$_2$)$_2$), 77 (5). Anal. Calcd for $C_{31}H_{49}NO_8P_2$ (625.7): C, 59.51; H, 7.89; N, 2.24; P, 9.90. Found: C, 59.54; H, 7.84; N, 2.20; P, 9.95.

5.2.2. Tetraethyl 2-(3,5-di-tert-butyl-2-hydroxyphenylamino)-2-(4-methoxyphenyl)ethane-1,1-diyl-diphosphonate, ***6a***

Colorless crystals yield: 71%, mp 193–195 °C (from MeOH). IR (cm^{-1}, KBr): ν_{max} 3464, 3348$_w$ (OH & NH), 1234, 1228 (2P=O, bonded), 1161, 1144 (2P–O–C). ^{1}H NMR [$CDCl_3$] ppm: 1.22, 1.31 (2dt, J_{H-H} = 7.2, $^4J_{P-H}$ = 5.6 Hz, 2× 6H, 4H_3CCOP), 1.35, 1.38 (2s, 2× 9H, (H_3C)$_3$C), 3.36 (s, 3H, H_3CO), 3.73 (dt, J_{H-H} = 9.3, $^2J_{P-H}$ = 14.4 Hz, 1H, H^aC–P$_2$), 4.00, 4.34 (2dq, J_{H-H} = 7.2, $^3J_{P-H}$ = 5.6 Hz, 2× 4H, 4H_2COP), 4.88 (dt, J_{H-H} = 9.3, $^3J_{P-H}$ = 6.2 Hz, 1H, H^b–C*), 7.05–7.62, 8.23 (m, 6H, *H*–Ar), 9.32 (s, br, 1H, *H*N), 9.98 (s (br), 1H, *H*O).^{13}C NMR [$CDCl_3$] ppm: 158.8, 151.5, 146.1, 138.8, 136.7, 134, 130.9, 122.9, 118.2, 113.1 (*C*–Ar), 64.5 (d, $^2J_{P-C}$ = 16.5 Hz, *C**HCP), 60.6 (d, $^2J_{P-C}$ = 10.5 Hz, *C*H$_2$OP), 55.1 (OCH$_3$), 44.2 (t, $^1J_{P-C}$ = 168.3 Hz, *C*–P$_2$), 37.4, 35.3

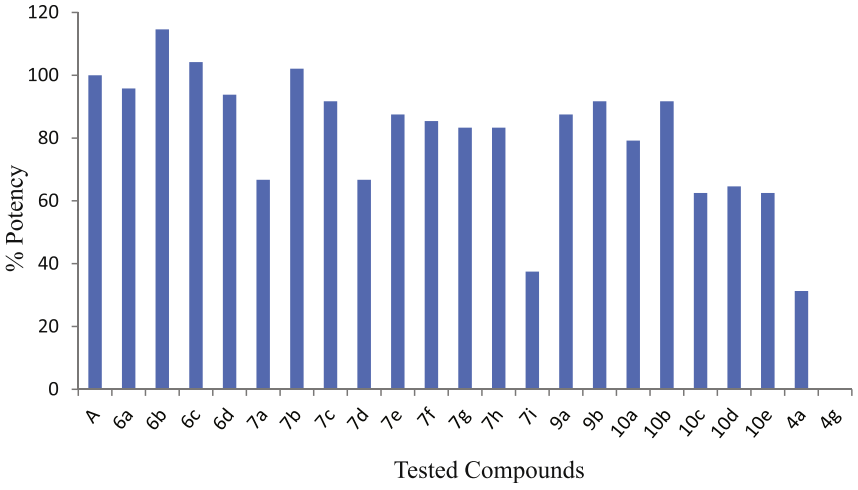

Fig. 1. Antiinflammatory activity of BPs **6a**–**d** and **7a**–**i**, and BP-acids **9a**,**b** and **10a**–**e**.

(2*C*(CH_3)$_3$), 31.2, 29.5 (2(CH_3)$_3$*C*),15.3 (d, $^3J_{P-C}$ = 7.5 Hz, *C*H_3COP). ^{31}P NMR [$CDCl_3$] ppm: 26.6, 31.3 (2d, $^2J_{P-P}$ = 26.4 Hz, P_2–C). EI-MS: in *m*/*z* (%): 625 (13) [M^+ − 2], 607 (23) [M^+ − 20 (2H + H_2O)], 576 (18) [M^+ − 51(2H + H_2O + OMe)], 439 (34) [M^+ − 188 (2H + H_2O + OMe + P(O) (OEt)$_2$)], 302 (100) [M^+ − 325(2H + H_2O + OMe+2{P(O)(OEt)$_2$})], 287 (46) (CH[P(O)(OEt)$_2$]$_2$), 137 (66) (P(O)(OEt)$_2$), 77 (56). Anal. Calcd for $C_{31}H_{51}NO_8P_2$ (627.7): C, 59.32; H, 8.19; N, 2.23; P, 9.87. Found: C, 59.39; H, 8.14; N, 2.18; P, 9.92.

5.3. Reaction of ***4b*** with ***5***

Reagents: (*E*)-2,4-Di-tert-butyl-6-(4-(dimethylamino)benzylideneamino)phenol, **4b** (1.3 g, 3.8 mmol), BP-reagent **5** (1.2 mL, 4.2 mmol), EtONa (0.2 g of Na, 9.1 mmol), and EtOH (20 mL). The product residue was chromatographed with *n*-hexane/$CHCl_3$ (6:4 v/v) to give **7b**, followed with *n*-hexane/$CHCl_3$ (1:1 v/v) to give **6b**.

5.3.1. Tetraethyl (5,7-di-tert-butyl-2-(4-dimethylaminophenyl)-2,3-dihydrobenzo[d]oxazol-2-yl)methylenediphosphonate, ***7b***

Colorless crystals yield: ≈7%, mp 133–135 °C (from cyclohexane). IR (cm^{-1}, KBr): ν_{max} 3350$_w$ (NH), 1236, 1226 (2P═O, bonded), 1164, 1079, (2P–O–C). ^{1}H NMR [$CDCl_3$] ppm: 1.12, 1.28 (2dt, J_{H-H} = 6.7, $^4J_{P-H}$ = 4.5 Hz, 2× 6H, 4H_3CCOP), 1.33, 1.47 (2s, 2× 9H, 2(H_3C)$_3$C), 3.36 (t, $^2J_{P-H}$ = 17 Hz, 1H, *H*C–P$_2$), 3.83, (s, 6H, (H_3C)$_2$N), 4.11, 4.22 (2dq, J_{H-H} = 6.7, $^3J_{P-H}$ = 5.8 Hz, 2× 4H, 4H_2COP), 6.97–7.76, 8.33 (m, 6H, *H*–Ar), 8.96 (s(br), 1H, *H*N). ^{13}C NMR [$CDCl_3$] ppm: 149.1, 146.2, 137.4, 134.7, 130.6, 125.3, 118.8, 117.8, 115.4, 110.6 (*C*–Ar), 61.2 (d, $^2J_{P-C}$ = 10.5 Hz, *C*H_2OP), 40.6 (N(*C*H_3)$_2$), 38 (d, $^1J_{P-C}$ = 173.3 Hz, *C*–P$_2$), 37, 31.7 (2 *C*(CH_3)$_3$), 31.2, 30.4 (2(CH_3)$_3$*C*), 15.4 (d, $^3J_{P-C}$ = 7.5 Hz, *C*H_3COP). ^{31}P NMR [$CDCl_3$] ppm: 24.8, 28.7 (2d, $^2J_{P-P}$ = 22.4 Hz, P_2–C). EI-MS: in *m*/*z* (%): 637 (14) [M^+ − 1], 593 (56) [M^+ − 45(H + N(Me)$_2$], 319 (28) [M^+ − 319(H + N(Me)$_2$ + 2{P(O)(OEt)$_2$})}, 306 (100) [M^+ − 332 (H + N(Me)$_2$ + CH[P(O)(OEt)$_2$]$_2$)], 287 (40) (CH[P(O)(OEt)$_2$]$_2$), 137 (46) (P(O)(OEt)$_2$), 77 (77). Anal. Calcd for $C_{32}H_{52}N_2O_7P_2$ (638.7): C, 60.17; H, 8.21; N, 4.39; P, 9.70. Found: C, 60.13; H, 8.15; N, 4.33; P, 9.77.

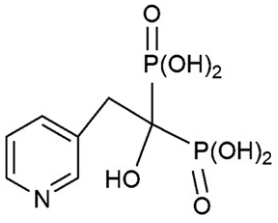

Structure 11. . Risedronate.

5.3.2. Tetraethyl 2-(3,5-di-tert-butyl-2-hydroxyphenylamino)-2-(4-dimethylaminophenyl)ethane-1,1-diyldiphosphonate, ***6b***

Colorless crystals, yield: 70%, mp 171–173 °C (from EtOH). IR (cm^{-1}, KBr): ν_{max} 3444, 3367 (OH & NH), 1242, 1219 (2P = O, bonded), 1050, 1034 (2P–O–C). ^{1}H NMR [$CDCl_3$] ppm: 1.22, 1.29 (2dt, J_{H-H} = 6.6, $^4J_{P-H}$ = 4.8 Hz, 2× 6H, 4H_3CC·OP), 1.37, 1.52 (2s, 2× 9H, 2(H_3C)$_3$C), 3.53 (s, 6H, *Me*$_2$N), 3.77 (dt, J_{H-H} = 9.5, $^2J_{P-H}$ = 15.6 Hz, 1H, H^aC–P$_2$), 4.05, 4.23 (2dq, J_{H-H} = 6.6, $^3J_{P-H}$ = 7.2 Hz, 2× 4H, 2H_2COP), 5.04 (dt, J_{H-H} = 9.5, $^3J_{P-H}$ = 6.2 Hz, 1H, H^b–*C), 7.02–7.67, 8.23 (m, 6H, *H*–Ar), 9.03 (s (br), 1H, *H*N), 10.19 (s (br), 1H, O*H*). ^{13}C NMR [$CDCl_3$] ppm: 151.2, 148.6, 146.6, 138.4, 136.8, 131.6, 129.5, 122.7, 114.4, 113.6 (*C*–Ar), 64.7 (d, $^2J_{P-C}$ = 13.6 Hz, C*HCP), 62.4 (d, $^2J_{P-C}$ = 11.3 Hz, *C*H_2OP), 47.6 (t, $^1J_{P-C}$ = 174.2 Hz, *C*–P$_2$), 39.5 [(CH_3)$_2$N], 37.2, 35.3 (2*C*(CH_3)$_3$), 31.6, 30.3 (2(CH_3)$_3$*C*),15.6 (d, $^3J_{P-C}$ = 7.5 Hz, *C*H_3COP). ^{31}P NMR [$CDCl_3$] ppm: 23.8, 27.7 (2d, $^2J_{P-P}$ = 32.4 Hz, P_2–C). EI-MS: in *m*/*z* (%): 638 (40) [M^+ − 2], 620 (28) [M^+ − 20(2H + H_2O)], 576 (23) [M^+ − 64 (2H + H_2O + NMe_2)], 439 (54) (M^+ − 201 (2H + H_2O + NMe_2+P(O)(OEt)$_2$)], 302 (100) (M^+ − 338 (2H + H_2O + NMe_2+2{P(O)(OEt)$_2$})], 287 (16) (CH[P(O)(OEt)$_2$]$_2$), 137 (36) (P(O)(OEt)$_2$), 77 (66). Anal. Calcd for $C_{32}H_{54}N_2O_7P_2$ (640.7): C, 59.99; H, 8.49; N, 4.37; P, 9.67. Found: C, 60.05; H, 8.43; N, 4.31; P, 9.74.

5.4. Reaction of ***4c*** with ***5***

Reagents: (*E*)-2,4-Di-tert-butyl-6-(4-fluorobenzylideneamino) phenol, **4c** (1.2 g, 3.8 mmol), BP-reagent **5** (1.2 mL, 4.2 mmol), EtONa (0.2 g of Na, 9.1 mmol), and EtOH (30 mL). The product residue was chromatographed with *n*-hexane/$CHCl_3$ (6:4 v/v) to give **7c**, followed with *n*-hexane/$CHCl_3$ (1:1 v/v) to give **6c**.

5.4.1. Tetraethyl (5,7-di-tert-butyl-2-(4-fluorophenyl)-2,3-dihydrobenzo[d]oxazol-2-yl)methylenediphosphonate, ***7c***

Colorless crystals, yield: ≈5%, mp 94–96 °C (from pentane). IR (cm^{-1}, KBr): ν_{max} 3340$_w$ (NH), 1236, 1226 (2P═O, bonded), 1154, 1097 (2P–O–C). ^{1}H NMR [$CDCl_3$] ppm: 1.13, 1.27(2dt, J_{H-H} = 6.5, $^4J_{P-H}$ = 4.3 Hz, 2× 6H, 4H_3CC·OP), 1.36, 1.57 (2s, 2× 9H, (H_3C)$_3$C), 2.96 (t, $^2J_{P-H}$ = 18.8 Hz, 1H, *H*C–P$_2$), 4.06, 4.17 (2dq, J_{H-H} = 6.5, $^3J_{P-H}$ = 5.6 Hz, 2× 4H, 4H_2COP), 7.17–7.86, 8.15, 8.17 (m, 6H, *H*–Ar), 9.04 (s (br), 1H, *H*N). ^{13}C NMR [$CDCl_3$] ppm: 164.6, 158.5, 146.2, 137.4,

132.3, 127.6, 120.2, 119.9, 118.6, 110.3 (*C*–Ar), 61.4 (d, $^2J_{P-C}$ = 10.5 Hz, *C*H_2OP), 38.2 (t, $^1J_{P-C}$ = 158.3 Hz, *C*–P_2), 37.3, 31.7 (2*C*$(CH_3)_3$), 31.2, 30.4 (2(*C*H_3)$_3$C), 15.4 (d, $^3J_{P-C}$ = 7.5 Hz, *C*H_3COP). ^{31}P NMR [$CDCl_3$] ppm: 26.6, 29.3 (2d, $^2J_{P-P}$ = 30.2 Hz, P_2–C). EI-MS: in *m*/*z* (%): 612 (21) [M^+ − 1], 593 (66) [M^+ − 20 (H + F)], 319 (33) (M^+ − 294 (H + F+2{P(O)(OEt)$_2$})], 306 (100) [M^+ − 307 (H + F + CH{P(O)(OEt)$_2$}$_2$)], 287 (16) (CH[P(O)(OEt)$_2$]$_2$), 137 (36) (P(O)(OEt)$_2$), 77 (86). Anal. Calcd for $C_{30}H_{46}FNO_7P_2$ (613.6): C, 58.72; H, 7.56; F, 3.10; N, 2.28; P, 10.10. Found: C, 58.76; H, 7.49; F, 3.15; N, 2.24; P, 10.17.

5.4.2. Tetraethyl 2-(3,5-di-tert-butyl-2-hydroxyphenylamino)-2-(4-fluorophenyl)ethane-1,1-diyldiphosphonate, **6c**

Colorless crystals, yield: 72%, mp 138–140 °C (from EtOH). IR (cm^{-1}, KBr): ν_{max} 3427, 3335$_w$ (OH & NH), 1238, 1222 (2P=O, bonded), 1085, 1066 (2P–O–C). ^{1}H NMR [$CDCl_3$] ppm: 1.16, 1.32 (2dt, J_{H-H} = 7.2, $^4J_{P-H}$ = 5.6 Hz, 2× 6 H, 4*H*$_3$CCOP), 1.36, 1.52 (2s, 2× 9H, 2(*H*$_3$C)$_3$C), 3.23 (dt, J_{H-H} = 9.6, $^2J_{P-H}$ = 16.1 Hz, 1H, *H*^{a}C–P_2), 4.11, 4.14 (2dq, J_{H-H} = 7.2, $^3J_{P-H}$ = 5.9 Hz, 2× 4H, 4*H*$_2$COP), 5.24 (dt, J_{H-H} = 9.6, $^3J_{P-H}$ = 7.6 Hz, 1H, *H*^{b}–C*), 7.06–7.77, 8.24 (m, 6H, *H*–Ar), 8.92 (s, br, 1H, *H*N), 9.58 (s (br), 1H, *H*O). ^{13}C NMR [$CDCl_3$] ppm: 163.8, 151.8, 146.1, 138.8, 136.4, 130.2, 123.4, 120.3, 119.8, 113.6 (*C*–Ar), 65.7 (d, $^2J_{P-C}$ = 11.8 Hz, C*HCP), 60.4 (d, $^2J_{P-C}$ = 11.3 Hz, *C*H_2OP), 46.8 (t, $^1J_{P-C}$ = 155.2 Hz, *C*–P_2), 37.2, 35.3 (2*C*$(CH_3)_3$), 31.6, 30.3 (2(*C*H_3)$_3$C),16.2 (d, $^3J_{P-C}$ = 7.2 Hz, *C*H_3COP). ^{31}P NMR [$CDCl_3$] ppm: 23.7, 25.8 (2d, $^2J_{P-P}$ = 31.1 Hz, P_2–C). EI-MS: in *m*/*z* (%): 613 (18) [M^+ − 2], 595 (21) [M^+ − 20 (2H + H_2O)], 576 (63) [M^+ − 39(2H + H_2O + F)], 439 (24) [M^+ − 176 (2H + H_2O + F + P(O)(OEt)$_2$)], 303 (100) (M^+ − 313 (2H + H_2O + F+2P(O)(OEt)$_2$)], 287 (16) (CH[P(O)(OEt)$_2$]$_2$), 137 (36) (P(O)(OEt)$_2$), 77 (86). Anal. Calcd for $C_{30}H_{48}FNO_7P_2$ (615.6): C, 58.53; H, 7.86; F, 3.09; N, 2.28; P, 10.06. Found: C, 58.49; H, 7.82; F, 3.11; N, 2.24; P, 10.12.

5.5. Reaction of **4d** with **5**

Reagents: (*E*)-2,4-Di-tert-butyl-6-(4-nitrobenzylideneamino) phenol, **4d** (1.3 g, 3.8 mmol), BP-reagent **5** (1.2 mL, 4.2 mmol), EtONa (0.2 g of Na, 9.1 mmol), and EtOH (30 mL). The product residue was chromatographed with *n*-hexane/$CHCl_3$ (6:4 v/v) to give **7d**, followed with *n*-hexane/$CHCl_3$ (1:1 v/v) to give **6d**.

5.5.1. Tetraethyl (5,7-di-tert-butyl-2-(4-nitrophenyl)-2,3-dihydrobenzo[d]oxazol-2-yl) methylenediphosphonate, **7d**

Straw yellow crystals, yield: ~5%, mp 164–165 °C (from EtOH). IR (cm^{-1}, KBr): ν_{max} 3334$_w$ (NH), 1242, 1226 (2P=O, bonded), 1056, 1044 (2P–O–C). ^{1}H NMR [$CDCl_3$] ppm: 1.14, 1.17 (2dt, J_{H-H} = 7.2, $^4J_{P-H}$ = 4.3 Hz, 2× 6H, 4*H*$_3$CC·OP), 1.35, 1.41 (2s, 2× 9H, 2(*H*$_3$C)$_3$C), 3.26 (t, $^2J_{P-H}$ = 18.5 Hz, 1H, *H*C–P_2), 3.97, 4.04 (2dq, J_{H-H} = 7.2, $^3J_{P-H}$ = 5.5 Hz, 2× 4H, 4*H*$_2$COP), 7.37, 7.69, 8.37, 8.42 (m, 6H, *H*–Ar), 9.06 (s(br), 1H, *H*N). ^{13}C NMR [$CDCl_3$] ppm: 148.3, 146.2, 137.4, 134.7, 132.6, 127.5, 126.4, 118.6, 115.4, 110.3 (*C*–Ar), 61.8 (d, $^2J_{P-C}$ = 10.5 Hz, *C*H_2OP), 42.6 (t, $^1J_{P-C}$ = 182.6 Hz, *C*–P_2), 37, 31.7 (2*C*$(CH_3)_3$), 31.2, 30.4 (2(*C*H_3)$_3$C), 15.4 (d, $^3J_{P-C}$ = 7.8 Hz, *C*H_3COP). ^{31}P NMR [$CDCl_3$] ppm: 25.6, 26.5 (2d, $^2J_{P-P}$ = 24.5 Hz, P_2–C). EI-MS: in *m*/*z* (%): 639 (27) [M^+ − 1], 593 (68) [M^+ − 47(H + NO_2], 319 (28) [M^+ − 321(H + NO_2+2{P(O)(OEt)$_2$})], 306 (100) [M^+ − 334(H + NO_2+CH[P(O)(OEt)$_2$]$_2$)], 287 (44) (CH[P(O)(OEt)$_2$]$_2$), 137 (36) (P(O)(OEt)$_2$), 77 (82). Anal. Calcd for $C_{30}H_{46}N_2O_9P_2$ (640.6): C, 56.24; H, 7.24; N, 4.37; P, 9.67. Found: C, 56.20; H, 7.28; N, 4.32; P, 9.73.

5.5.2. Tetraethyl 2-(3,5-di-tert-butyl-2-hydroxyphenylamino)-2-(4-nitrophenyl)ethane-1,1-diyldiphosphonate, **6d**

Straw yellow crystals, yield: 70%, mp 160–166 °C (from MeCN). IR (cm^{-1}, KBr): ν_{max} 3445, 3331$_w$ (OH & NH), 1238, 1222 (2P=O, bonded), 1101, 1064 (2P–O–C). ^{1}H NMR [$CDCl_3$] ppm: 1.16, 1.24 (2dt, J_{H-H} = 6.6, $^4J_{P-H}$ = 4.5 Hz, 2× 6H, 4*H*$_3$CC·OP), 1.37, 1.40 (2s, 2× 9H, (*H*$_3$C)$_3$C), 3.50 (dt, J_{H-H} = 9.0, $^2J_{P-H}$ = 15.6 Hz, 1H, *H*^{a}C–P_2), 4.07, 4.12 (2dq, J_{H-H} = 6.6, $^3J_{P-H}$ = 6.0 Hz, 2× 4H, 2*H*$_2$COP), 5.44 (dt, J_{H-H} = 9.0, $^3J_{P-H}$ = 6.4 Hz, 1H, *H*^{b}–*C), 7.37–7.69, 8.34 (m, 6H, *H*–Ar), 8.88 (s (br), 1H, *H*N), 10.49 (s (br), 1H, O*H*). ^{13}C NMR [$CDCl_3$] ppm: 151.8, 145.6, 137.6, 134.6, 133.4, 129.4, 127.4, 123.5, 122.8, 114.4 (*C*–Ar), 66.3 (d, $^2J_{P-C}$ = 14.7 Hz, C*HCP), 61.6 (d, $^2J_{P-C}$ = 9.7 Hz, *C*H_2OP), 45.7 (t, $^1J_{P-C}$ = 188.4 Hz, *C*–P_2), 37.5, 36.6 (2*C*$(CH_3)_3$), 31.8, 30.4 (2(*C*H_3)$_3$C), 15.6 (d, $^3J_{P-C}$ = 8.2 Hz, *C*H_3COP). ^{31}P NMR [$CDCl_3$] ppm: 26.3, 28.6 (2d, $^2J_{P-P}$ = 34.6 Hz, P_2–C). EI-MS: in *m*/*z* (%): 640 (30) [M^+ − 2], 622 (28) [M^+ − 20(2H + H_2O)], 576 (20) [M^+ − 66(2H + H_2O + NO_2)], 439 (46) (M^+ − 203 (2H + H_2O + NO_2+P(O)(OEt)$_2$)], 302 (100) (M^+ − 340 (2H + H_2O + NO_2+2{P(O)(OEt)$_2$})], 287 (25) (CH[P(O)(OEt)$_2$]$_2$), 137 (32) (P(O)(OEt)$_2$), 77 (72). Anal. Calcd for $C_{30}H_{48}N_2O_9P_2$ (642.6): C, 56.07; H, 7.53; N, 4.36; P, 9.64. Found: C, 56.11; H, 7.47; N, 4.32; P, 9.69.

When the above reactions (**4a**–**d** + **5**) were carried out in methanol solution containing sodium (Na) using the same amounts, and in the presence of 4.1 mmol of 2,3 dichloro-5,6-dicyanobenzoquinne (DDQ) at r.t. for ≈6–10 h (TLC), BPs **7a**–**d** were obtained after the usual working up, as a sole reaction products. Yields: **7a** (76%), **7b** (73%), **7c** (76%), and **7d** (80%).

5.6. General procedure of **7e**–**i**

Following the general procedure, a mixture of 9.12 mmol of Na, 4.2 mmol of **5**, 4.1 mmol of DDQ, and 3.8 mmol of the Shiff-bases **4e**–**i** in 20 mL of MeOH was heated under reflux for 8–10 h. The product mixture was chromatographed with *n*-hexane/$CHCl_3$ to give **7e** (6:4 v/v), **7f** (3:7 v/v), **7g** (8:2 v/v), **7h** (3:7 v/v), and **7i** (8:2 v/v).

5.6.1. Tetraethyl (5,7-di-tert-butyl-2-(4-hydroxyphenyl)-2,3-dihydrobenzo[d]oxazol-2-yl)methylene-diphosphonate, **7e**

Colorless needles, yield: 75%, mp 148–150 °C (from EtOH). IR (cm^{-1}, KBr): ν_{max} 3350 (br) (OH, NH), 1233, 1225 (2P=O, bonded), 1075, 1024 (2P–O–C). ^{1}H NMR [$CDCl_3$] ppm: 1.26, 1.32 (2dt, J_{H-H} = 7.4, $^4J_{P-H}$ = 4.3 Hz, 2× 6H, 4*H*$_3$CC·OP), 1.33, 1.44 (s, 2× 9H, (*H*$_3$C)$_3$C), 3.14 (t, $^2J_{P-H}$ = 17.5 Hz, 1H, *H*C–P_2), 4.07, 4.11 (2dq, J_{H-H} = 7.4, $^3J_{P-H}$ = 6.5 Hz, 2× 4H, 4*H*$_2$COP), 7.39–7.45, 7.81 (m, 6H, *H*–Ar), 8.95, 9.24 (2s (br), 2× 1H, *H*N&O*H*). ^{13}C NMR [$CDCl_3$] ppm: 156.3, 148.2, 146.2, 137.4, 131.5, 126.7, 120.6, 118.6, 115.3, 110.6 (*C*–Ar), 62.4 (d, $^2J_{P-C}$ = 10.5 Hz, *C*H_2OP), 44.8 (t, $^1J_{P-C}$ = 178.3 Hz, *C*–P_2), 37, 31.7 (2*C*$(CH_3)_3$), 31.2, 30.4 (2(*C*H_3)$_3$C), 15.9 (d, $^3J_{P-C}$ = 7.5 Hz, *C*H_3COP). ^{31}P NMR [$CDCl_3$] ppm: 30.3, 31.7 (2d, $^2J_{P-P}$ = 20.6 Hz, P_2–C). EI-MS: in *m*/*z* (%): 610 (33) [M^+ − 1], 593 (26) [M^+ − 18(H + OH)], 319 (28) [M^+ − 292(H + OH+2{P(O) (OEt)$_2$})], 306 (100) [M^+ − 305(H + OH + CH[P(O)(OEt)$_2$]$_2$)], 287 (29) (CH [P(O) (OEt)$_2$]$_2$), 137 (55) (P(O)(OEt)$_2$), 77 (52). Anal. Calcd for $C_{30}H_{47}NO_8P_2$ (611.6): C, 58.91; H, 7.75; N, 2.29; P, 10.13. Found: C, 59.09; H, 7.79; N, 2.25; P, 10.16.

5.6.2. Tetraethyl (5,7-di-tert-butyl-2-(4-chlorophenyl)-2,3-dihydrobenzo[d]oxazol-2-yl)methylene-diphosphonate, **7f**

Colorless needles, yield: 82%, mp 102–104 °C (from cyclohexane). IR (cm^{-1}, KBr): ν_{max} 3350$_w$ (NH), 1236, 1223 (2P=O, bonded), 1055, 1029 (2P–O–C). ^{1}H NMR [$CDCl_3$] ppm: 0.88, 1.25 (2dt, J_{H-H} = 6.2, $^4J_{P-H}$ = 3.8 Hz, 2× 6H, 4*H*$_3$CC·OP), 1.46, 1.53 (s, 2× 9H, (*H*$_3$C)$_3$C), 3.32 (t, $^2J_{P-H}$ = 20.4 Hz, 1H, *H*C–P_2), 4.29, 4.42 (2dq, J_{H-H} = 6.2, $^3J_{P-H}$ = 6.1 Hz, 2× 4H, 4*H*$_2$COP), 7.31–7.70, 8.17 (m, 6H, *H*–Ar), 8.96 (s (br), 1H, *H*N). ^{13}C NMR [$CDCl_3$] ppm: 148.1, 146.2, 139.6, 139.2, 137.4, 134.8, 128, 118.6, 115.4, 110.6 (*C*–Ar), 61.6 (d, $^2J_{P-C}$ = 10.5 Hz, *C*H_2OP), 40.7 (t, $^1J_{P-C}$ = 144.3 Hz, *C*–P_2), 37, 31.7 (2 *C*$(CH_3)_3$), 31.2, 30.4 (2(*C*H_3)$_3$C), 16.4 (d, $^3J_{P-C}$ = 8.2 Hz, *C*H_3COP). ^{31}P NMR [$CDCl_3$] ppm: 27.4, 30.6 (2d, $^2J_{P-P}$ = 22.8 Hz, P_2–C). EI-MS: in *m*/*z* (%): 631(21) [M^++2], 629 (7) [M^+], 628 (32) [M^+ − 1], 593 (26) [M^+ − 36 (H + Cl)], 319 (28) [M^+ − 310(H + Cl + 2{P(O)

$(OEt)_2$)}), 306 (100) [M^+ − 323(H + Cl + CH [P(O)$(OEt)_2]_2$)], 287 (31) (CH[P(O) $(OEt)_2]_2$), 137 (68) (P(O)$(OEt)_2$), 77 (67). Anal. Calcd for $C_{30}H_{46}ClNO_7P_2$ (630.1): C, 57.19; H, 7.36; Cl, 5.63; N, 2.22; P, 9.83. Found: C, 57.24; H, 7.30; Cl, 5.58; N, 2.27; P, 9.87.

5.6.3. Tetraethyl (5,7-di-tert-butyl-2-(3-chlorophenyl)-2,3-dihydrobenzo[d]oxazol-2-yl)methylene-diphosphonate, ***7g***

Colorless crystals, yield: 78%, mp 88–90 °C (from pentane). IR (cm^{-1}, KBr): ν_{max} 3350_w (NH), 1240, 1224 (2P═O, bonded), 1164, 1079 (2P–O–C). ^{1}H NMR [$CDCl_3$] ppm: 0.98, 1.17 (2dt, J_{H-H} = 7.2, $^4J_{P-H}$ = 4.3 Hz, 2× 6H, 4H_3CCOP), 1.38, 1.54 (2s, 2× 9H, (H_3C)$_3$C), 3.25 (t, $^2J_{P-H}$ = 18.8 Hz, 1H, *H*C–P$_2$), 4.05, 4.12 (2dq, J_{H-H} = 7.2, $^3J_{P-H}$ = 6.4 Hz, 2× 4H, 4H_2COP), 7.34–7.67, 8.19–8.23 (m, 6H, *H*–Ar), 9.06 (s (br), 1H, *H*N). ^{13}C NMR [$CDCl_3$] ppm: 147.9, 146.2, 142.3, 142.2, 137.8, 134.9, 127.2, 125.6, 115.6, 109.7 (*C*–Ar), 61.7 (d, $^2J_{P-C}$ = 10.5 Hz, *C*H$_2$OP), 44.0 (t, $^1J_{P-C}$ = 142.3 Hz, *C*–P$_2$), 37, 31.7 (2*C*(CH$_3$)$_3$), 31.2, 30.4 (2(*C*H$_3$)$_3$C), 15.4 (d, $^3J_{P-C}$ = 7.5 Hz, *C*H$_3$COP). ^{31}P NMR [$CDCl_3$] ppm: 26.8, 30.8 (2d, $^2J_{P-P}$ = 28.4 Hz, P_2–C). EI-MS: in *m*/*z* (%): 631(18) [M^+ + 2], 629 (6) [M^+], 628 (35) [M^+ − 1], 306 (100) [M^+ − 323 (H + Cl + CH[P(O)$(OEt)_2]_2$)]. Anal. Calcd for $C_{30}H_{46}ClNO_7P_2$ (630.1): C, 57.19; H, 7.36; Cl, 5.63; N, 2.22; P, 9.83. Found: C, 57.25; H, 7.32; Cl, 5.67; N, 2.17; P, 9.88.

5.6.4. Tetraethyl (5,7-di-tert-butyl-2-(2-chlorophenyl)-2,3-dihydrobenzo[d]oxazol-2-yl)methylenediphosphonate, ***7h***

Colorless crystals, yield: 76%, mp 113–115 °C (from pentane). IR (cm^{-1}, KBr): ν_{max} 3355_w (NH), 1235, 1225 (2P═O, bonded), 1164, 1079 (2P–O–C). ^{1}H NMR [$CDCl_3$] ppm: 0.89, 1.05 (2dt, J_{H-H} = 6.8, $^4J_{P-H}$ = 3.8 Hz, 2× 6H, 4H_3CCOP), 1.38, 1.53 (2s, 2× 9H, 2(H_3C)$_3$C), 3.47 (t, $^2J_{P-H}$ = 18.8 Hz, 1H, *H*C–P$_2$), 4.12, 4.20 (2dq, J_{H-H} = 6.8, $^3J_{P-H}$ = 6.7 Hz, 2× 4H, 4H_2COP), 6.99–7.67, 8.15–8.24 (m, 6H, *H*–Ar), 9.07 (s (br), 1H, *H*N). ^{13}C NMR [$CDCl_3$] ppm: 148.1, 146.2, 137.1, 134.2, 130.3, 128.4, 127.7, 118.4, 115.2, 110.3 (*C*–Ar), 62.1 (d, $^2J_{P-C}$ = 14.5 Hz, *C*H$_2$OP), 39.2 (t, $^1J_{P-C}$ = 158.3 Hz, *C*–P$_2$), 37, 31.7 (2 *C*(CH$_3$)$_3$), 31.2, 30.4 (2(*C*H$_3$)$_3$C), 16.4 (d, $^3J_{P-C}$ = 8.7 Hz, *C*H$_3$COP). ^{31}P NMR [$CDCl_3$] ppm: 29.5, 31.4 (2d, $^2J_{P-P}$ = 26.3 Hz, P_2–C). EI-MS: in *m*/*z* (%): 631 (24) [M^++2], 629 (8) [M^+], 628 (36) [M^+ − 1], 306 (100) [M^+ − 323(H + Cl + CH[P(O)$(OEt)_2]_2$)]. Anal. Calcd for $C_{30}H_{46}ClNO_7P_2$ (630.1): C, 57.19; H, 7.36; Cl, 5.63; N, 2.22; P, 9.83. Found: C, 57.13; H, 7.29; Cl, 5.56; N, 2.26; P, 9.90.

5.6.5. Tetraethyl (5,7-di-tert-butyl-2-(2,5-dimethoxyphenyl)-2,3-dihydrobenzo[d]oxazol-2-yl)methylenediphosphonate, ***7i***

Colorless crystals, yield: 79%, mp 128–130 °C (from CH_2Cl_2). IR (cm^{-1}, KBr): ν_{max} 3342_w (NH), 1235, 1224 (2P═O, bonded), 1078, 1045 (2P–O–C). ^{1}H NMR [$CDCl_3$] ppm: 1.13, 1.18 (2dt, J_{H-H} = 6.8, $^4J_{P-H}$ = 4.6 Hz, 2× 6H, 4H_3CC·OP), 1.35, 1.40 (2s, 2× 9H, 2(H_3C)$_3$C), 3.22 (t, $^2J_{P-H}$ = 16.5 Hz, 1H, *H*C–P$_2$), 3.75, 3.81 (2s, 2× 3H, 2H_3CO), 4.14, 4.20 (2dq, J_{H-H} = 6.8, $^3J_{P-H}$ = 5.8 Hz, 2× 4H, 4H_2COP), 7.23–7.88, 8.34 (m, 5H, *H*–Ar), 9.81 (s (br), 1H, *H*N). ^{13}C NMR [$CDCl_3$] ppm: 159.4, 149.9, 146.2, 137.3, 136.4, 123.1, 118.5, 115.7, 112.3, 108.9 (*C*–Ar), 61.2 (d, $^2J_{P-C}$ = 10.5 Hz, *C*H$_2$OP), 55.8, 55.3 (2*C*H$_3$O), 39.8 (t, $^1J_{P-C}$ = 152.3 Hz, *C*–P$_2$), 37.2, 31.7 (2*C*(CH$_3$)$_3$), 31.2, 30.4 (2(*C*H$_3$)$_3$C), 15.6 (d, $^3J_{P-C}$ = 8.2 Hz, *C*H$_3$COP). ^{31}P NMR [$CDCl_3$] ppm: 31.3, 26.4 (2d, $^2J_{P-P}$ = 30.6 Hz, P_2–C). EI-MS: in *m*/*z* (%): 654 (48) [M^+ − 1], 592 (26) [M^+ − 63(H + 2{OMe})], 318 (28) [M^+ − 337(H + 2{OMe} + 2 {P(O)$(OEt)_2$)}), 305 (100) [M^+ − 350(H + 2{OMe}) + CH–[P(O)$(OEt)_2]_2$)], 287 (55) (CH[P(O)$(OEt)_2]_2$), 137 (34) (P(O)$(OEt)_2$), 77 (84). Anal. Calcd for $C_{32}H_{51}NO_9P_2$ (655.7): C, 58.62; H, 7.84; N, 2.14; P, 9.45. Found: C, 58.67; H, 7.83; N, 2.08; P, 9.51.

5.7. General procedure of BP-acids ***9a,b****, and* ***10a–e***

Bisphosphonate **6b**,**c**, **7b**,**c**, and **7f**–**h** (0.5 g) was dissolved in 15 mL of *conc* HCl, and the mixture was heated under reflux for ≈8 h (TLC). After concentrating the product mixture to its half, under reduced pressure, the crude material was diluted with AcOEt and water and then stirred for 30 min. The layers were separated, and the aqueous layer was evaporated to dryness. The precipitate was collected and dried to give the corresponding BP-acids **9a**,**b** and **10a**–**e**.

5.7.1. 2-(3,5-Di-tert-butyl-2-hydroxyphenylamino)-2-(4-dimethylaminophenyl)ethane-1,1-diyldiphosphonic acid, ***9a***

White substance, yield: 67%, mp > 300 °C (from EtOH). IR (cm^{-1}, KBr): ν_{max} 3420–3332 (P–OH, NH), 1233–1219 (P═O, bonded). ^{1}H NMR [D_2O] ppm: 1.37, 1.40 (2s, 2× 9H, 2(H_3C)$_3$C), 2.44 (dt, J_{H-H} = 11.4, $^2J_{P-H}$ = 15.3 Hz, 1H, H^aC–P$_2$), 2.82 (s, 6H, 2(H_3C)$_2$N), 5.26 (dt, J_{H-H} = 11.4, $^3J_{P-H}$ = 7.2 Hz, 1H, H^b–C), 7.16–7.78, 8.23 (m, 6H, *H*–Ar). ^{31}P NMR [D_2O] ppm: 21.2, 22.7. EI-MS: in *m*/*z* (%): 522 (24) [M^+ − 6]. Anal. Calcd for $C_{24}H_{38}N_2O_7P_2$ (528.5): C, 54.54; H, 7.25. Found: C, 54.50; H, 7.18.

5.7.2. 2-(3,5-Di-tert-butyl-2-hydroxyphenylamino)-2-(4-fluorophenyl)ethane-1,1-diyldiphosphonic acid, ***9b***

White substance, yield: 70%, mp >300 °C (from EtOH), IR: ν_{max}, cm^{-1}: 3420–3332 (P–OH, NH), 1235–1222 (P═O, bonded). ^{1}H NMR [D_2O] ppm: 1.35, 1.38 (2s, 2× 9H, 2(H_3C)$_3$C), 2.48 (dt, J_{H-H} = 11.4, $^2J_{P-H}$ = 18.8 Hz, 1H, H^aC–P$_2$), 5.20 (dt, J_{H-H} = 11.4, $^3J_{P-H}$ = 5.9 Hz, 1H, H^b–C), 7.14–7.77, 8.20 (m, 6H, *H*–Ar). ^{31}P NMR [D_2O] ppm: 22.2, 24.7. EI-MS: in *m*/*z* (%): 497 (30) [M^+ − 6]. Anal. Calcd for $C_{22}H_{32}FNO_7P_2$ (503.4): C, 52.49; H, 6.41. Found: C, 52.44; H, 6.45.

5.7.3. (5,7-di-tert-butyl-2-(4-(dimethylamino)phenyl)-2,3-dihydrobenzo[d]oxazol-2-yl)methylene-diphosphonic acid, ***10a***

White substance, yield: 65%, mp >300 °C (from EtOH). IR (cm^{-1}, KBr): ν_{max} 3415–3329 (P–OH, NH), 1233–1220 (P═O, bonded). ^{1}H NMR [D_2O] ppm: 1.38, 1.52 (2s, 2× 9H, 2(H_3C)$_3$C), 2.40 (t, $^2J_{P-H}$ = 16.4 Hz, 1H, *H*C–P$_2$), 2.80 (s, 6H, 2(H_3C)$_2$N), 7.14–7.72, 8.10 (m, 6H, *H*–Ar). ^{31}P NMR [D_2O] ppm: 21.2, 23.5. EI-MS: in *m*/*z* (%): 520 (40) [M^+ − 6]. Anal. Calcd $C_{24}H_{36}N_2O_7P_2$ (526.5): C, 54.75; H, 6.89. Found: C, 54.71; H, 6.84.

5.7.4. (5,7-Di-tert-butyl-2-(4-fluorophenyl)-2,3-dihydrobenzo[d]oxazol-2-yl)methylenediphosphonic acid, ***10b***

White substance, yield: 73%, mp >300 °C (from EtOH). IR (cm^{-1}, KBr): ν_{max} 3424–3335 (P–OH, NH), 1230–1225 (P═O). ^{1}H NMR [D_2O] ppm: 1.36, 1.57 (2s, 2× 9H, 2(H_3C)$_3$C), 2.50 (t, $^2J_{P-H}$ = 18.8 Hz, 1H, *H*C–P$_2$), 7.18–7.68, 8.15 (m, 6H, *H*–Ar). ^{31}P NMR [D_2O] ppm: 23.2, 25.6. EI-MS: in *m*/*z* (%): 495 (32) [M^+ − 6]. Anal. Calcd for $C_{22}H_{30}FNO_7P_2$ (501.4): C, 52.70; H, 6.03. Found: C, 52.75; H, 6.81.

5.7.5. (5,7-Di-tert-butyl-2-(4-chlorophenyl)-2,3-dihydrobenzo[d]oxazol-2-yl)methylenediphosphonic acid, ***10c***

White substance, yield: 66%, mp >300 °C (from EtOH). IR (cm^{-1}, KBr): ν_{max} 3425–3336 (P–OH, NH), 1233–1220 (P═O). ^{1}H NMR [D_2O] ppm: 1.35, 1.40 (2s, 2× 9H, 2(H_3C)$_3$C), 2.44 (t, $^2J_{P-H}$ = 17.2 Hz, 1H, *H*C–P$_2$), 7.20–7.60, 8.12 (m, 6H, *H*–Ar). ^{31}P NMR [D_2O] ppm: 24.2, 26.4. EI-MS: in *m*/*z* (%): 511 (45) [M^+ − 6]. Anal. Calcd for $C_{22}H_{30}ClNO_7P_2$ (517.9): C, 51.02; H, 5.84. Found: C, 51.07; H, 5.59.

5.7.6. (5,7-Di-tert-butyl-2-(3-chlorophenyl)-2,3-dihydrobenzo[d]oxazol-2-yl)methylenediphosphonic acid, ***10d***

White substance, yield: 72%, mp >300 °C (from EtOH). IR (cm^{-1}, KBr): ν_{max} 3426–3328 (P–OH, NH), 1236–1219 (P═O). ^{1}H NMR [D_2O] ppm: 1.32, 1.40 (2s, 2× 9H, 2(H_3C)$_3$C), 2.38 (t, $^2J_{P-H}$ = 15.4 Hz, 1H, *H*C–P$_2$), 7.18–7.50, 8.10 (m, 6H, *H*–Ar). ^{31}P NMR [D_2O] ppm: 22.2, 24.6. EI-MS: in *m*/*z* (%): 511 (35) [M^+ − 6]. Anal. Calcd for $C_{22}H_{30}ClNO_7P_2$ (517.9): C, 51.02; H, 5.84. Found: C, 51.06; H, 5.82.

5.7.7. (5,7-Di-tert-butyl-2-(3-chlorophenyl)-2,3-dihydrobenzo[d] oxazol-2-yl)methylenediphosphonic acid, ***10e***

White substance, yield: 72%, mp >300 °C (from EtOH). IR (cm^{-1}, KBr): ν_{max} 3426–3327 (P–OH, NH), 1230–1220 (P=O). ^{1}H NMR [D_2O] ppm: 1.37, 1.53 (2s, 2× 9H, 2(H_3C)$_3$C), 2.42 (t, $^2J_{P-H}$ = 15.6 Hz, 1H, *H*C–P_2), 6.80–7.40, 8.10 (m, 6H, *H*–Ar). ^{31}P NMR [D_2O] ppm: 24.5, 26.6. EI-MS: in *m*/*z* (%): 511 (42) [M^+ − 6]. Anal. Calcd for $C_{22}H_{30}ClNO_7P_2$ (517.9): C, 51.02; H, 5.84. Found: C, 51.04; H, 5.80.

5.8. Bioassays

5.8.1. Lipophilicity HPLC determination (capacity factor K/ calculated log K)

The HPLC separation module Waters Alliance 2695 XE and Waters Photodiode Array Detector 2996 (Waters Corp., Milford, MA, U.S.A.) were used. The Chromatographic Column Symmetry® C_{18} 5 μm, 4.6 × 250 mm, Part No. WAT054275, (Waters Corp., Milford, MA, U.S.A.) was used. The HPLC separation process was monitored by Millennium32® Chromatography Manager Software, Waters 2004 (Waters Corp., Milford, MA, U.S.A.). The mixture of MeOH p.a. (90.0%) and H_2O-HPLC – Mili-Q Grade (10.0%) was used as a mobile phase. The total flow of the column was 1.0 ml/min, injection 30 μl, column temperature 45 °C and sample temperature 10 °C. The detection wavelength 210 nm was chosen. The KI methanolic solution was used for the dead time (T_D) determination. Retention times (T_R) were measured in minutes. The capacity factors *K* were calculated using the Millennium32® Chromatography Manager Software according to the formula $K = (T_R - T_D)/T_D$, where T_R is the retention time of the solute, whereas T_D denotes the dead time obtained via an unretained analyte. The log *K* values of the individual compounds, calculated from the capacity factor *K*, are shown in Table 1. All values displayed as mean ± s.d. Superscript letters denote equivalent means determined by pairwise comparison (Dunnett T3, $p < 0.05$).

5.8.2. Lipophilicity calculations

Converting the logarithm of the partition coefficient for *n*-octanol/water (log *K*) to the lipophilcity coefficient (Log *P*) was calculated using the programs CS ChemOffice Ultra ver. 10.0 (CambridgeSoft, Cambridge, MA, USA) and ACD/LogP ver. 12.0 (Advanced Chemistry Development Inc., Toronto, Canada). Clog *P* values (the logarithm of *n*-octanol/water partition coefficient based on established chemical interactions) were generated by means of CS ChemOffice Ultra ver. 10.0 (CambridgeSoft, Cambridge, MA, U.S.A.) software. The results are shown in Table 1.

5.9. Pharmacology

5.9.1. Antitumor activity screening

Anti-tumor potency of the new BPs **6a**–**d**, **7a**–**i**, and BP-acids **9a**,**b**, and **10a**–**e**, in addition to the substrates **4a** and **4g** was tested at a dose of 10 μM utilizing 16 different human tumor cell lines, representing breast, ovarian, prostate and liver cancer using adriamycin as a reference standard according to the reported methods [24,25]. The human tumor cell lines of the cancer screening panel are grown in RPMI 1640 medium containing 5% fetal bovine serum and 2 mL-glutamine. For a typical screening experiment, cells are inoculated in 96-well-microtiter plates in 100 mL at plating densities ranging from 5000 to 40,000 cells/well depending on the doubling time individual cell lines. After cell inoculation, the microtiter plates are incubated at 37 °C, 5% CO_2, 95% air and 100% relative humidity for 24 h prior to addition of experimental tested compounds. After 24 h, two plates of each cell lines are fixed in situ with trichloroacetic acid (TCA), to represent a measurement of the cell population for each cell line at the time of the tested compound addition (time zero, *Tz*). Experimental tested compounds are solubilized in dimethyl sulfoxide at 400-fold the desired final maximum test concentration and stored frozen prior to use. At the time of the tested compound addition, an aliquot of frozen concentrate is thawed and diluted to twice the desired final maximum test concentration with complete medium containing 50 mg/mL gentamicine. Additional four, 10-fold or ½ log serial dilutions are made to provide a total of five tested compound concentrations (10^{-4} to 10^{-8} M concentrations) plus control. Aliquots of 100 mL of these different tested compound dilutions are added to the appropriate microtiter wells already containing 100 μL of medium, resulting in the required final concentrations.

Following the tested compound addition, the plates are incubated for an additional 48 h at 37 °C, 5% CO_2, 95% air and 100% relative humidity. For adherent cells, the assay is terminated by the addition of cold TCA. Cells are fixed in situ by the gentle addition of 50 μL of cold 50% (w/v) TCA (final concentration, 10% TCA) and incubated for 60 min at 4 °C. The supernatant is discarded, and the plates are washed four times with tap water and air dried. Sulforhodamine B (SRB) solution (100 μL) at 0.4% (w/v) in 1% acetic acid is added to each well, and plates are incubated for 10 min at room temperature. After staining, unbound dye is removed by washing four times with 1% acetic acid and the plates are air dried. Bound stain is subsequently solubilized with 10 μM trizma base, and the absorbance is read on an automated plate read at a wavelength of 515 nm. For cells suspension, the methodology is the same except that the assay is terminated by fixing settled cells at the bottom of the wells by gently adding 50 μL of 80% TCA (final concentration, 16% TCA). Using the seven absorbance measurements (*Tz*), control growth (*C*) and test growth in the presence of the tested compound at the five concentration levels (*Ti*), the percentage growth is calculated at each of the tested compound concentration levels.

Percentage growth inhibition is calculated as follows:

$$[(Ti - Tz)/(C - Tz)] \times 100$$

for concentrations for which $Ti \geq Tz$.

$[(Ti - Tz)/Tz)] \times 100$ for concentration for which $Ti < Tz$.

Growth inhibition of 50% (GI_{50}) is calculated from:

$[(Ti - Tz)/[(C - Tz) \times 100 = 50\%$ (GI_{50}), which is the tested compound concentration resulting in a 50% reduction in the net protein increase (as measured in SRB staining) in control cells during the compound incubation. Table 2 represents the observed percentage growth of each cell line treated with a certain tested compound relative to control cell line experiments.

5.9.2. Delayed type hypersensitivity granuloma

Groups of 10 female albino mice (25 g) were sensitized with an emulsion of methylated bovine serum albumin (mBSA) in saline with Freund's incomplete adjuvant and dextran by sc injection over the inguinal lymph node. Three weeks later, hydroxyapatite (HA) discs 6-mm diameter) soaked in mBSA solution (30 mg/mL saline) were implanted sc in the dorsum of the mice (two discs, bilaterally). All drugs were prepared as solutions, suspensions, or emulsions, and the pH was adjusted to 7.4 with 0.1 M NaOH. Each mouse received compound in a volume of 0.1 mL/10 g body weight sc in the scruff of the neck. Dosing commenced on the day of implantation of the mBSA soaked discs and was continued thereafter on a daily basis until day nine, when the mice were euthanized. The granulomatous lesions were then excised and both wet and dry tissue weights measured. Results were analyzed by Student's paired *t* test. The results are displayed in Table 3.

The antiinflammatory activity was expressed as percentage inhibition of edema volume in the treated animals in comparison with the control group.

$$\%\,\text{Inhibition of edema} = \frac{(V_c - V_t)}{V_c} \times 100$$

where V_c and V_t are the volumes of edema for the control and tested substance-treated animal groups, respectively, while potency of the tested compounds was calculated regarding risedronate, reference standard, treated group according to the following equation:

$$\%\text{Potency} = \frac{\%\text{Edema inhibition of tested compound treated group}}{\%\text{Edema inhibition of risedronate treated group}} \times 100$$

Acknowledgments

Authors like to thank the Central Lab, School of Pharmacy, Alexandria University, Egypt, and NY Cancer Institute, NY, USA for carrying out the pharmacological screening.

Appendix A. Supplementary data

Supplementary data related to this article can be found at http://dx.doi.org/10.1016/j.ejmech.2012.09.032.

References

[1] H. Fleisch, Bisphosphonates: a new class of drugs in diseases of bone and calcium metabolism, in: P.F. Baker (Ed.), In Handbook of Experimental Pharmacology, vol. 83, Springer, Berlin/Heidelberg, 1988, pp. 441–465.
[2] H. Fleisch, Bisphosphonates in Bone Disease: From the Laboratory to the Patient, The Parathenone Publishing Group Inc, New York, 1995.
[3] A.J. Yates, G.A. Rodan, Alendronate and osteoporosis, Drug Discov. Today 3 (1998) 69–78.
[4] T. Anada, Y. Takeda, Y. Honda, K. Sakurai, O. Suzuki, Synthesis of calcium phosphate-binding liposome for drug delivery, Bioorg. Med. Chem. Lett. 19 (2009) 4148–4150.
[5] W.K. Siestema, F.H. Ebetino, Bisphosphonates in development for metabolic bone disease, Expert Opin. Investig. Drugs 3 (1994) 1255–1276.
[6] S.A. Gittens, G. Bansal, R.F. Zernicke, H. Uludag, Designing proteins for bone targeting, Adv. Drug Deliv. Rev. 57 (2005) 1011–1036.
[7] H. Hirabayashi, J. Fujisaki, Phosphonated rifamycins and uses thereof for the prevention and treatment of bone and joint infections, Clin. Pharmacokinet. 42 (2003) 1319–1330.
[8] D. Wang, S.C. Miller, P. Kopeckova, J. Kopecek, Bone-targeted macromolecular therapeutics, Adv. Drug Deliv. Rev. 57 (2005) 1049–1076.
[9] T.V. den Wyngaert, M.T. Huizing, E. Fossion, J.B. Vermorken, Bisphosphonates in oncology: rising stars or fallen heroes, The Oncologist 14 (2009) 181–191.
[10] A. Lipton, R.L. Theriault, G.N. Hortobagyi, J. Simeone, R.D. Knight, K. Mellars, D.J. Reitsma, M. Heffernan, J. Seaman, Pamidronate prevents skeletal complications and is effective palliative treatment in women with breast carcinoma and osteolytic bone metastases, J. Cancer 88 (2000) 1082–1090.
[11] T. Yoneda, A. Sasaki, C. Dustan, P.J. William, F. Bauss, Y.A. De Clerck, G.R. Mundy, Inhibition of osteolytic bone metastasis of breast cancer by combined treatment with the bisphosphonate ibandronate and tissue inhibitor of the matrix metalloproteinase-2, J. Clin. Invest. 99 (1997) 2509–2517.
[12] M. Busch, M. Rave-Frank, A. Hille, E. Duhmke, Influence of clodronate on breast cancer cells in vitro, Eur. J. Med. Res. 3 (1998) 427–431.
[13] J.E. Brown, E.C. Robert, The role of bisphosphonates in breast cancer: the present and future role of bisphosphonates in the management of patients with breast cancer, Breast Cancer Res. 4 (2002) 24–29.
[14] R.A. Baron, R. Tavaré, A.C. Figueiredo, K.M. Baewska, B.A. Kashemirov, C.E. McKenna, F.H. Ebetino, A. Taylor, M.J. Rogers, F.P. Coxon, M.C. Seabra, Phosphono-carboxylates inhibit the second geranylgeranyl addition by rab geranylgeranyl transferase, Biol. Chem. 284 (2009) 6861–6868.
[15] L.I. Plotkin, J.I. Aguirre, S. Kousteni, S.C. Manolagas, T. Bellido, Bisphosphonates and estrogens inhibit osteocyte apoptosis via distinct molecular mechanisms downstream of extracellular signal-regulated kinase activation, J. Biol. Chem. 280 (2005) 7317–7325.
[16] W.M. Abdou, R.E. Khidre, A.A. Kamel, Elaborating on efficient anti-proliferation agents of cancer cells and anti-inflammatory-based on *N*-bisphosphonic acids, Arch. Pharm. Chem. Life Sci. 345 (2012) 123–136.
[17] W.M. Abdou, A.A. Kamel, R.E. Khidre, A. Geronikaki, M.T. Ekonomopoulou, Synthesis of 5- and 6-*N*- heterocyclic methylenebisphosphonate derivatives of cytogenetic activity in normal human lymphocyte cultures, Chem. Biol. Drug Des. 79 (2012) 719–730.
[18] A.A. Kamel, W.M. Abdou, A. Geronikaki, Inhibitory effect of novel *S*, *N*-bisphosphonates on some carcinoma cell lines, osteoarthritis, and chronic inflammation, Eur. J. Med. Chem. 51 (2012) 239–249.
[19] T. Hartmann, J. Schmitt, Liphilicity-beyond octanol/water: a comparison of modern technologies, Drug Disc. Today Technol. 1 (2004) 431–439.
[20] P. Wils, A. Warnery, V. Phung-Ba, S. Legrain, D. Scherman, High lipophilicity decreases drug transport across intestinal epithelial cells, J. Pharmacol. Exp. Ther. 269 (1994) 654–658.
[21] J. Vinsová, K. Cermáková, A. Tomecková, M. Cecková, J. Jampílek, P. Cermák, J. Kunes, M. Dolezal, F. Staud, Synthesis and antimicrobial evaluation of new 2-substituted 5,7-di-tert-butylbenzoxazoles, Bioorg. Med. Chem. 14 (2006) 5850–5865.
[22] J. Jampilek, J. Vinsova, J. Kaderavkova, in: J.A. Seijas, V.T.M. Pilar (Eds.), From Proceedings of the International Electronic Conference on Synthetic Organic Chemistry, 10th, November 1–30 (2006), a003/10.
[23] D. Walker, J.D. Herbert, 2,3-Dichloro-5,6-dicyanobenzoqinone and its reactions, Chem. Rev. 67 (1966) 153–195.
[24] T. Kitamura, M. Itoh, T. Noda, M. Matsuura, K. Wakabayashi, Combined effects of cyclooxygenase-1 and cyclooxygenase-2 selective inhibitors on intestinal tumorigenesis in adenomatous polyposis coli gene knockout mice, Int. J. Cancer 109 (2004) 576–580.
[25] M.R. Boyd, K.D. Paull, Some practical considerations and applications of the National Cancer Institute in vitro anticancer drug discovery screen, Drug Dev. Res. 34 (1995) 91–109.
[26] R.A. Nugent, M. Murphy, S.T. Schlachter, C.J. Dunn, R.J. Smith, N.D. Staite, L.A. Galinet, S.K. Shields, D.G. Aspar, K.A. Richard, N.A. Rohloff, Pyrazoline bisphosphonate esters as novel antiinflammatory and antiarthritic agents, J. Med. Chem. 36 (1993) 134–139.
[27] C.J. Dunn, L.A. Galinet, A.J. Gibbons, S.K. Shields, Murine delayed type hypersensitivity granuloma: an improved model for the identification and evaluation of different classes of antiarthritic drugs, Int. J. Immunopharmacol. 12 (1990) 899–904.